Meteorol Atmos Phys 99, 1–16 (2008)
DOI 10.1007/s00703-006-0238-z
Printed in The Netherlands

Meteorology and Atmospheric Physics

Department of Meteorology, School of Ocean and Earth Science and Technology, University of Hawaii at Manoa, Honolulu, Hawaii, USA

Climate variation and prediction of rapid intensification in tropical cyclones in the western North Pacific

B. Wang and **X. Zhou**

With 13 Figures

Received September 4, 2006; revised October 8, 2006; accepted December 27, 2006
Published online: December 12, 2007

Summary

One of the greatest challenges in tropical weather forecasting is the rapid intensification (RI) of the tropical cyclone (TC), during which its one-minute maximum sustained wind speed increases at least 30 knots per 24 hours. Here we identify and elucidate the climatic conditions that are critical to the frequency and location of the RI on annual, intraseasonal, and interannual time scales. Whereas RI and formation share common environmental preferences, we found that the percentage of TCs with RI varies annually and from year to year. In August, only 30% of TC actually experiences RI, in contrast to the annual maximum of 47% in November. The proportion of RI in July–September is higher during El Niño years (53%) than the corresponding one in the La Niña years (37%). Three climate factors may contribute to the increase in the proportion of RI: the southward shift in the monthly or seasonal mean location of the TC formation, the increase in the low-level westerly meridional shear vorticity, and the decrease in northerly vertical shear. When the mean latitude of TC formation increases, the mixed-layer heat content decreases while TC's inertial stability increases; both are more detrimental to the RI than to TC formation because the RI requires large amount of latent heat energy being extracted efficiently from the ocean mixed layer and requires accelerated low-level radial inflow that carries latent heat reaching the inner core region.

We further demonstrate that the RI frequency in the Philippine Sea and South China Sea can be predicted 10 to 30 days in advance based on the convective anomalies in the equatorial western Pacific (5° S–5° N, 130°–150° E) on intraseasonal time scale. The Niño 3.4 SSTA in June is a potential predictor for the peak TC season (July–September) RI activity in the southeast quadrant of the western North Pacific (0–20° N, 140–180° E).

The RI is an essential characteristic of category 4 and 5 hurricanes and super typhoons because all category 4 and 5 hurricanes in the Atlantic basin and 90% of the super typhoons in the western North Pacific experience at least one RI process in their life cycles. Over the past 40 years, the annual total of RI in the western North Pacific shows pronounced interdecadal variation but no significant trend. This result suggests that the number of supper typhoons has no upward trend in the past 40 years. Our results also suggest that when the mean latitude, where the tropical storms form, shifts southward (either seasonally or from year to year) the proportion of super typhoon or major hurricane will likely increase. This shift is determined by large scale circulation change rather than local SST effects. This idea differs from the current notion that increasing SST can lead to more frequent occurrence of category 4 or 5 hurricanes through local thermodynamics.

1. Introduction

The forecasting of intensity changes in tropical cyclones (TCs) has strikingly large errors during TC rapid intensification (RI). This is, in part, attributed to our inadequate understanding of the physical mechanisms governing TC inner-core processes and their interaction with the large-scale environment (Gross, 2001; DeMaria et al, 2002). Efforts have been made to identify

favorable synoptic conditions for RI. Over the Atlantic Ocean, Kaplan and DeMaria (2003) found that RIs are embedded in the regions with the following characteristics: weaker vertical wind shear; favorable upper-level forcing from troughs or cold low, warmer SST; and higher lower-troposphere relative humidity. In the western North Pacific, Ventham and Wang (2007) found that very rapid intensification is characterized by lower-level monsoon confluence, and the onset of RI is marked by a split of the upper-level flows into the mid-latitude westerlies to the north and into the sub-equatorial trough to the south of the TCs. Both investigations suggest that environmental flows play critical roles in determining RI on a synoptic time scale. However, the climate variability of the RI on intraseasonal to interannual time scales has not been studied.

Thus far, a majority of the previous investigations conducted on low-frequency variability of TCs have primarily focused on TC formation on a seasonal time scale (Gray, 1968; 1998; Holland, 1995), an interannual time scale (e.g., Gray, 1984; Chan, 1985; Lander, 1994a; Chen et al, 1998; Landsea, 2000; Wang and Chan, 2002), and an intraseasonal time scale (e.g., Nakazawa, 1988; Hendon and Liebmann, 1994; Maloney and Hartmann, 2000; 2001; Hall et al, 2001; Harr, 2006). An interesting question that has arisen is whether the large-scale environment also modulates frequencies and locations of the RI on various low-frequency time scales and what are the differences in environmental conditions between RI and TC formation.

The importance of studying the climate control of RI cannot be overemphasized. The RI is an essential characteristic of category 4 and 5 hurricanes, defined by one-minute maximum sustained wind speed equals or greater than 115 knots (59 m/s). Over the western Pacific the counterpart of category 4 and 5 hurricane is called super typhoon. All category 4 and 5 hurricanes in the Atlantic basin and 90% of the equivalent-strength typhoons (as will be seen shortly) in the western North Pacific experience at least one RI process in their life cycles. Therefore, better understanding the climate control of RI will shed light on the mechanisms responsible for the climate change in the supper typhoons.

Unfortunately, few works have been undertaken to study climate variability of the RI except a few climatological studies. Brand (1973) noticed a southeastward movement of the preferred areas for RI from August to October. Holliday and Thompson (1979) examined climatological features of RI based on 79 cases during the period of 1956–1976 over the western North Pacific. A majority of RI occurrences was concentrated in a 5-degree band between 15° N and 20° N beginning approximately 550 km west of Luzon and stretching to near the northern Marianas. The researchers suggested that TC development over warm oceans with SST not lower than 28 °C is a necessary feature but not a prerequisite for rapid deepening. These early results were based on a study of limited samples before 1976, when it is believed that TC intensity data was less reliable; further, their interests were focused only on annual variation.

Here, we examine the seasonal, intraseasonal, interannual and interdecadal variability of RI and explore how and to what extent the low-frequency variations of the large-scale environment impact the frequencies and locations of TCs RI. In particular, we are concerned with the similarity and difference between the large-scale control of RI and TC formation. The knowledge gained from such an analysis may help to improve our understanding of the RI processes and provide important background and useful predictors for improving our seasonal and intraseasonal prediction of RI activity.

Section 2 describes the dataset used in the present study and discusses the definition of RI. The general characteristics and seasonal distribution of RI compared with TC formation are provided in Sect. 3. The intraseasonal and interannual variability of the RI are presented in Sects. 4 and 5, respectively. Section 6 examines the possibility for making intraseasonal and seasonal prediction of RI. Conclusions and discussions are offered in the last section.

2. Datasets and definition of rapid intensification (RI)

The TC best-track data used in the present study were obtained from the Joint Typhoon Warning Center website, which record location and intensity of all TCs (including tropical depression) over the western North Pacific in six-hour intervals over a 40-year period, from 1965 to 2004.

The year of 1965 was selected as the starting year because the satellite monitoring of weather events first became routine at that time, so the data are believed to be more reliable than earlier records. The values of T-number based on subjective analysis of cloud patterns were used to determine TC intensity (Dvorak, 1975). Errors that arise from the subjective analysis are inevitable. But, this type of error is not deemed a serious problem for study of the RI because the value of the T-number increases rapidly during a RI. Nevertheless, one should bear in mind that uncertainties are induced by subjective technique in the absence of other measures. Other data sets used include sea surface temperature (SST) anomalies in the Niño-3.4 (5° S–5° N, 120° W–170° W) extracted online from the Climate Prediction Center website, the outgoing longwave radiation (OLR) dataset from the National Oceanic and Atmospheric Administration (NOAA) polar orbiting satellites, and the wind fields derived from the National Centers for Environmental Prediction–National Center for Atmospheric Research (NCEP/NCAR) reanalysis data.

The definition of RI is diverse in the existing literature. Brand (1973) considered a 50-knot increase in 24 hours as RI, whereas Holliday and Thompson (1979) used the abrupt reduction of minimum sea level pressure by 42 hPa/day as RI, which represents the top 25% of typhoon stage intensifiers. A threshold of 30 knots/day, which is equivalent to 95% percentile of intensity change, was employed by Kaplan and DeMaria (2003) for defining RI over the North Atlantic basin. Ventham and Wang (2007) used 35 and 40 knots per 24 hours as RI thresholds for weak and strong tropical storms, respectively, because the top percentile of intensification rate varies with initial intensity of TCs.

We found that the threshold of 30 knots/24 hours is equivalent to a 94 percentile of 24-hour intensity changes for all TCs over the WNP. This threshold depends weakly on the initial intensity and seems to be adequate for defining RI. Further, to avoid ambiguity in determining the onset and duration of the RI processes, we define RI as satisfying the following criteria: The increase of the maximum wind speed reaches at least (a) 5 knots in the first 6 hours, (b) 10 knots in the first 12 hours, and (c) 30 knots in 24 hours. While the criterion (c) is most crucial for defining an occurrence of RI, criteria (a) and (b) ensure that the initial time and location of a RI process are unambiguously determined. After a RI process starts, the time at which the three criteria are no longer met is defined as the end of the RI process. For the same TC, if RI occurs more than once, the second RI is termed as "Re-RI." The location of RI is determined by the first occurrence of RI if it occurs more than once.

3. Seasonal variation

On average, about ten TCs experienced at least one RI process each year over the western North Pacific east of 120° E, and of those, about one-forth underwent an additional Re-RI process. The number of TC with RI accounts for about 37% of all TCs. This ratio is higher than that over the Atlantic basin (31%) (Kaplan and DeMaria, 2003). About 65% of the typhoons and 90% of the intense typhoons (> 115 knots) underwent at least one RI process during their lifespans. These ratios are close to those of the Atlantic hurricanes, for which 60% of hurricanes and 100% of category 4 and 5 hurricanes underwent RI (Kaplan and DeMaria, 2003).

Preferred regions of RI are found roughly in a rectangular region (8° N–20° N, 125° E–155° E; Fig. 1). About 57% of RI TCs occur in this core region. The region of largest interannual variation (standard deviation exceeding 1.0 per 5×5 degree grid) tends to concur with the climatological mean maximum. The total variance within the core region of RI accounts for 52% of the total interannual variance. Note that the core re-

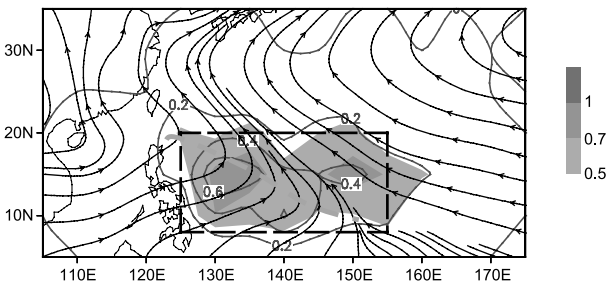

Fig. 1. Climatological mean distribution of the frequency of rapid intensification (RI). The contours denote the annual number of *initial* RI that occurred in each $5° \times 5°$ grid. The shading denotes the standard deviation of interannual variation. The boxed region outlines the core region of RI and its large interannual variations. Also shown are the July–August–September–October mean 850 hPa streamlines

gion of RI and its interannual variations display two centers: A major center (0.7 per 5×5 degree grid per year) around 15° N and 130° E and a secondary center extend eastward about 20 degrees of longitude to 150° E. Note also that the major center coincides with the climatological monsoon tough, while the secondary center is located to the northeast of the monsoon trough. Over the northern South China Sea, the frequency of TS occurrence is nearly as high as that over the Philippine Sea (figure not shown, but see, for instance, Wu and Wang, 2004); but, the occurrence of RI over the northern South China Sea is much fewer than that in the Philippine Sea (Fig. 1).

Some of the basic statistics regarding RI are given in this paragraph without showing figures for brevity. The frequencies of RI and Re-RI vary with their initial intensities. The maximum frequency of RI is found for the initial intensity of 35 knots, while the maximum frequency of Re-RI events shows two peaks at 45 knots and 75 knots. The average lifespan for RI processes is 36 hour, and almost a quarter of RI processes persists only 24 hours and only 3.6% of RI lasts more than 60 hours. On average a RI process results in a total of 55 knots increase in the maximum wind speed. RI processes with a total of 30–35-knot increase account for about 1/3 of all RI scenarios. A few extremely strong RI processes can accelerate more than 90 knots. The reasons for these extremely long-lasting and strongest RI processes deserve further case studies. To compare the variability of RI with TC formation, we will focus on RI TCs only.

The majority (84%) of the RI samples appear during July through November, with a peak in September (Fig. 2a). Seasonal distribution of RI bears a resemblance to that of TC formation except that TC formation peaks in August while

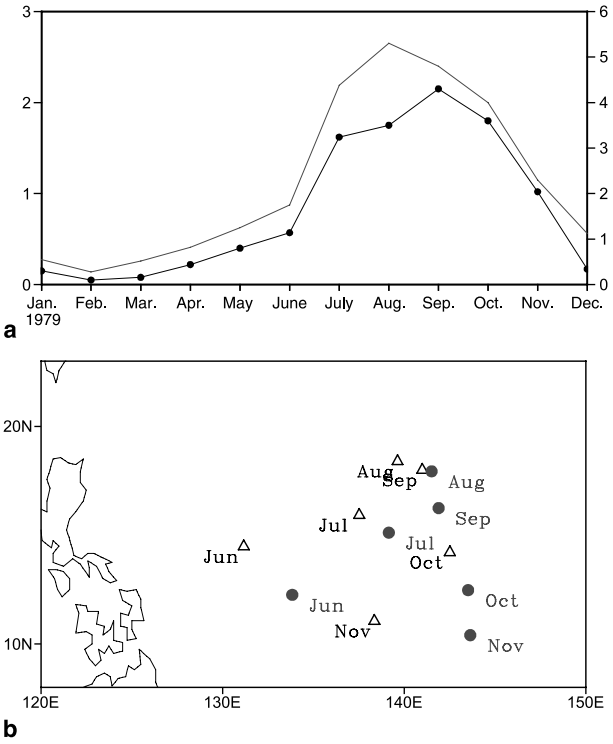

Fig. 2a. Seasonal distribution of the number of RI (black line with closed circle) and TC formation (thin line) averaged over the period 1965–2004; (**b**) seasonal shift in the monthly mean positions of TC RI (triangles) and formation (solids)

RI peaks in September. The monthly mean location of RI migrates northeastward from June to September and retreats equatorward after September (Fig. 2b). This seasonal march resembles that of TC formation except that the RI is positioned northwestward to its counterpart of TC formation, which results from the overall northwestward TC movement.

We note, however, that the ratio of rapidly intensifying TC to the total number of TC shows a very different seasonal distribution. The maximum ratio is seen in November (47%) while a

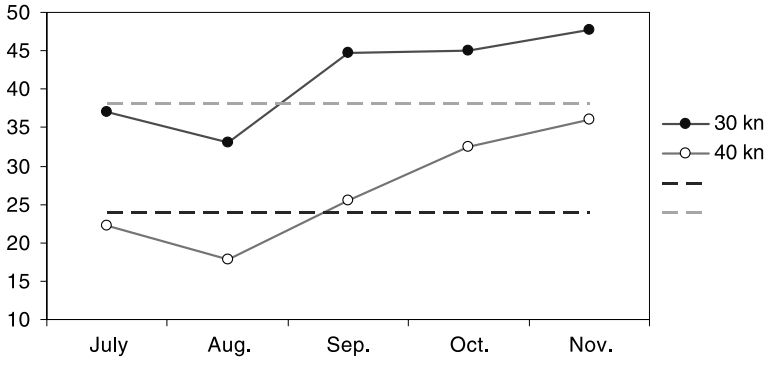

Fig. 3. The ratio of the number of TCs with RI to the total number of TCs formed over the WNP (solid). The line marked with an open circle represents a more restricted RI definition, using a threshold value of 40 knots per 24 hours. The dashed line represents the corresponding annual mean numbers (see text for more detail)

minimum (30%) is seen in August (Fig. 3). This was previously noticed but not explained (Brand, 1973; Holliday and Thompson, 1979). Further, Brand (1973) found that when the RI threshold changes from 50 knots/day to 40 knots/day, the minimum in August disappears. He speculated that a 40-knot increase was seemingly more common in August. Different from Brand (1973), we found that when the intensification criterion of 40 knots/24 hours is used, the minimum RI ratio (19%) remains in August and the maximum ratio (37%) remains in November (Fig. 3). Thus, the seasonal variation of the RI percentage is not sensitive to the RI definition.

August is the month that has the greatest number of TCs, but the ratio of RI to the total number of TC formations is the lowest in the July–November season. Why do the TCs formed in November have a greater chance of rapidly intensifying than those formed in August? Although TCs occur in a broad area over the WNP, a large percentage of them are concentrated in certain preferred regions, which vary from month to month (Fig. 2b). About 85% of the total RI cases occurred in a region spanning from 120° E to 160° E and in a 15-degree latitude band centered at the monthly mean position of RI. The environmental mean states in the regions between 120° E and 160° E are deemed important for understanding the RI.

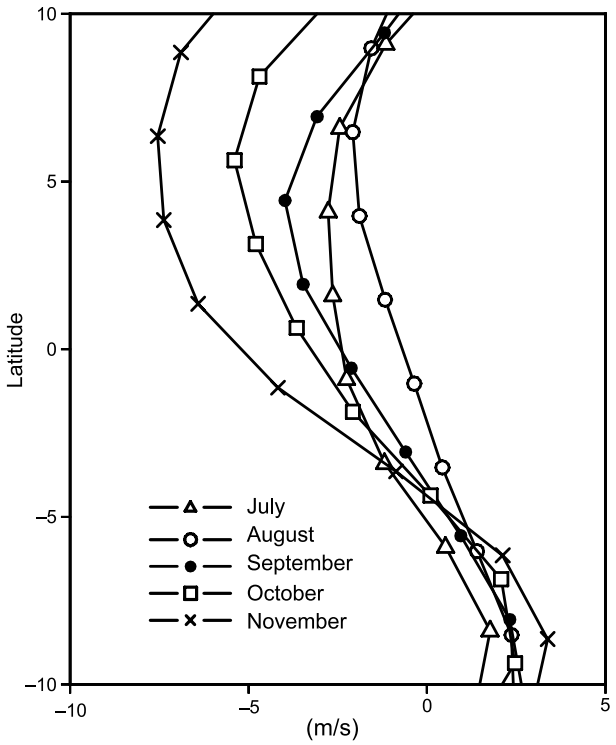

Fig. 4. Latitudinal variations of the climatological monthly mean zonal wind velocity at 850 mb averaged between 120° E and 160° E. Note that the origin in the latitude axis denotes the latitude of the monthly mean position of RI in each calendar month. See text for more detailed explanation

We found that the low-level meridional shear of zonal wind of the time mean state may explain why TCs that form in November have more frequent RI than those that form in August. Figure 4 presents the latitudinal variation of 850 hPa zonal wind averaged between 120° E and 160° E. The zonal wind has a minimum cyclonic shear in August but a maximum cyclonic shear in November. The result here suggests that a large low-level, environmental cyclonic shear of zonal mean wind can increase the chance of RI.

Why does the low-level cyclonic shear favor RI? We speculate that a zonal environmental flow with low-level cyclonic shear provides a quasi-stationary wavenumber-two forcing (Li and Wang, 1996), which may excite radially propagating inner-core asymmetric eddies. These eddies can enhance TC symmetric circulation and contribute to RI by subsequent axisymmetrization, which has been proposed by Montgomery and Enagonio (1998).

In addition to the aforementioned mechanism, there is perhaps another factor for explaining the relatively ineffective RI in August. The RI of TCs in August occurs nearly 8° latitude north of that in November (Fig. 2b). Bister (2001) showed that a weak warm-core mesoscale vortex takes twice the time to develop into a hurricane at 30° N than that at 10° N. It was suggested that the increase of inertial stability due to an increasing Coriolis parameter would weaken intensification rate (DeMaria and Pickle, 1988). The low-level inflow of a high-latitude vortex cannot reach the inner core region as quickly as can a low-latitude vortex. Therefore, the intensification occurs more slowly.

4. Intraseasonal variation

Previous studies have found that TCs tend to develop upon the arrival of super-cloud clusters associated with intraseasonal oscillation (ISO; Nakazawa, 1988; Hendon and Liebmann, 1994; Maloney and Hartmann, 2000; 2001; Hall et al, 2001). Liebmann et al (1994) found that nearly

twice as many formations occur during the wet phase of ISO as during the dry phase in the western Pacific and Indian Oceans. They attributed this to an increase in meso- and synoptic-scale convective activity brought about by ISO and the associated low-level cyclonic relative vortices and convergence anomalies that appear poleward and westward of the large-scale convective anomaly. Recently, by examining the linkage between the temporal clustering of TCs and Madden-Julian Oscillation (MJO), Harr (2006) found that in active MJO years, there is a statistically significant reduction in the probability of TC activity during the inactive convective phases and a statistically significant increase during active convective phases.

Of interest is the investigation of whether RI is also modulated by the ISO. To this end, a critical element of the study is to adequately define ISO activity over the western North Pacific. Liebmann et al (1994) used the minimum 35–95 day band-pass-filtered (bpf) OLR anomalies to identify wet phases of the ISO. With such a definition, however, the ISO signal itself would partially come from contributions from TC activity (Hsu et al, 2006). To avoid this type of ambiguity in the present study, we have used the WNP monsoon circulation index (WNPMI) as a measure of ISO. The WNPMI is defined by Wang and Fan (1999) as the following:

$$\mathrm{WNPMI} = \mathrm{U850}(5{-}15^\circ\,\mathrm{N}, 100{-}130^\circ\,\mathrm{E}) - \mathrm{U850}(20{-}30^\circ\,\mathrm{N}, 110{-}140^\circ\,\mathrm{E}).$$

This north–south differential 850 hPa zonal wind index reflects not only the strength of the tropical westerly monsoon over the Indo-China Peninsula, the South China Sea and Philippine (5–15° N, 100–130° E) but also the strength of the easterlies on the southern flank of the WNP subtropical high in the region (20–30° N, 110–140° E). Both the monsoon westerly and subtropical ridge are major systems affecting the WNP TC activity. Wang et al (2001) have shown that the WNPMI represents the dominant mode of interannual variability in the wind anomalies over the WNP and East Asian monsoon region (5–50° N, 100–145° E). It turns out that the 30–60 day band-pass-filtered (bpf) WNPMI can represent the ISO in the WNP and can define the

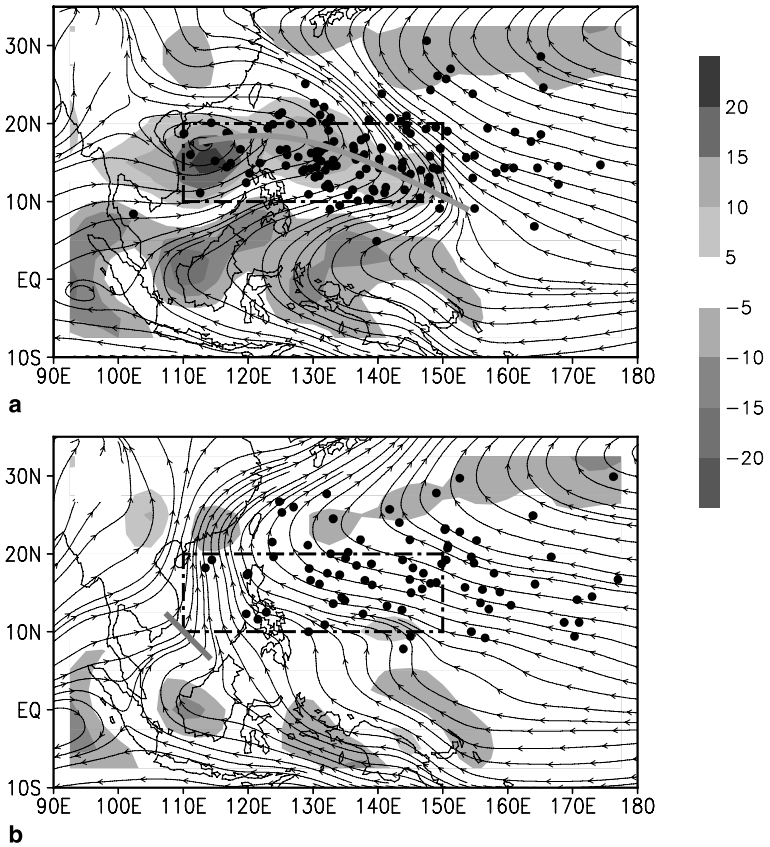

Fig. 5. The composite 850 hPa wind (streamlines) and vorticity (shading) fields for (**a**) positive (WNPMI > 1 m/s, enhanced monsoon trough) and (**b**) negative (WNPMI < −1 m/s, relaxed monsoon trough) phases of ISO during July–August–September–October. Dots represent locations of the first occurrence of RI reported. The dashed box highlights regions in which the largest differences between dry and wet phases of ISO are observed. The thick curves represent the location of the monsoon trough

onset of the South China Sea summer monsoon (Wang et al, 2004).

To determine the impact of the ISO on the RI, we performed a composite analysis for the ISOs positive and negative phases based on a 30–60-day filtered WNPMI. Figure 5 shows the number of occurrences of RI during positive (WNPMI$>$ 1 m/s) and negative (WNPMI<-1 m/s) phases of ISO for the July–October period from 1965 to 2004. A positive phase implies an enhanced WNP monsoon trough (Fig. 5a), and a negative phase implies a suppressed one (Fig. 5b). The composite low-level wind fields in these two extreme phases show a sharp contrast in the large-scale enhanced cyclonic vorticity in the positive phase and a reduced cyclonic vorticity in the negative phase within and to the northeast of the climatological monsoon trough region.

During the positive phases of ISO, the enhanced monsoon trough shifts northeastward of the climatological position (Fig. 5a). The subtropical ridge extends eastward and northward, with its ridgeline around 30° N. The equatorial buffer zone and associated northward cross-equatorial flows as well as the southwest monsoons are all considerably strengthened. Such circulation changes favor RI occurring in the Philippine Sea and northern South China Sea (i.e., the region bounded by 10–20° N, 110–150° E). In sharp contrast, during a negative ISO phase, the monsoon trough and the southwest monsoon flows disappear, and the subtropical high extends southwestward with a ridgeline tilting from (20° N, 120° E) to (25° N, 150° E) (Fig. 5b). As a result, the RI in the region (10–20° N, 110–150° E) amounts to 92 during the positive phases of ISO and only 36 in the negative phases, yielding a ratio of 2.6 (Table 1). The statistic significance of the differences in these two phases is tested by computing the Z statistic (Jones et al, 2004). The null hypothesis here is that the ratio in the composite positive phases is the same as that in the negative phases. A Z-value greater than 2.32 implies that the null hypothesis must be rejected, and the differences in the ratio between the positive and negative phases of ISO are statistically significant at the 99% confidence level. In comparison, TCs formed during positive and negative phases are 164 and 67, respectively, yielding a ratio of close to 2.4 (Table 1). The result here suggests that both the suppressed and enhanced TC formations share common favorable factors with those for RI.

Table 1. Contrast in the numbers of the rapid intensified TC and tropical depression (TD) between the positive and negative phases of ISO. The statistics were made for the key region of ISO in the western North Pacific (110–150° E, 10–20° N) and during the July through October (JASO) season for the period 1965–2004. The ISO phases were determined by the WNP monsoon circulation index (see text for explanation). A Z value larger than 2.32 implies that the differences between the wet and dry phases are statistical significance at the 99% confidence level

	WNPMI>1	WNPMI<-1	Normal	Total	Z
RI	92	36	55	183	3.2
TD	164	67	91	322	4.2

5. Interannual variation

5.1 Impacts of ENSO on RI

The number of TC formations in both the Atlantic and Pacific Oceans was closely modulated by El Niño-Southern Oscillation (ENSO) (Gray, 1984; Lander, 1994a; Chen et al, 1998; Landsea, 2000). In the WNP, ENSO affects the locations of tropical storm (TS) formation but does not significantly influence the total number of formations (Lander, 1994a; Chen et al, 1998). The latter differs from the Atlantic basin, where the total number of TC formation is affected by ENSO. However, the lifespan of tropical storm during warm events (seven days) is much longer than in the cold years (about four days) (Wang and Chan, 2002). As such, the frequency of the occurrence of tropical storm during warm years is much higher than in the cold years, even though the total number of TC formations is about the same. In summary, over the North Pacific, a strong El Niño event induces low-level cyclonic shear and an upper-level anomalous anticyclone over the western North Pacific, and a strong La Niña event induces low-level anticyclonic shear and an upper-level anomalous cyclone; both significantly alter TC formation locations, lifespan, track, and frequency of occurrence. Such anomalous large-scale circulation is expected to modulate RI as well. The following discussion focuses on the RI in the peak season, which includes July, August, and September (JAS). To better understand the difference in

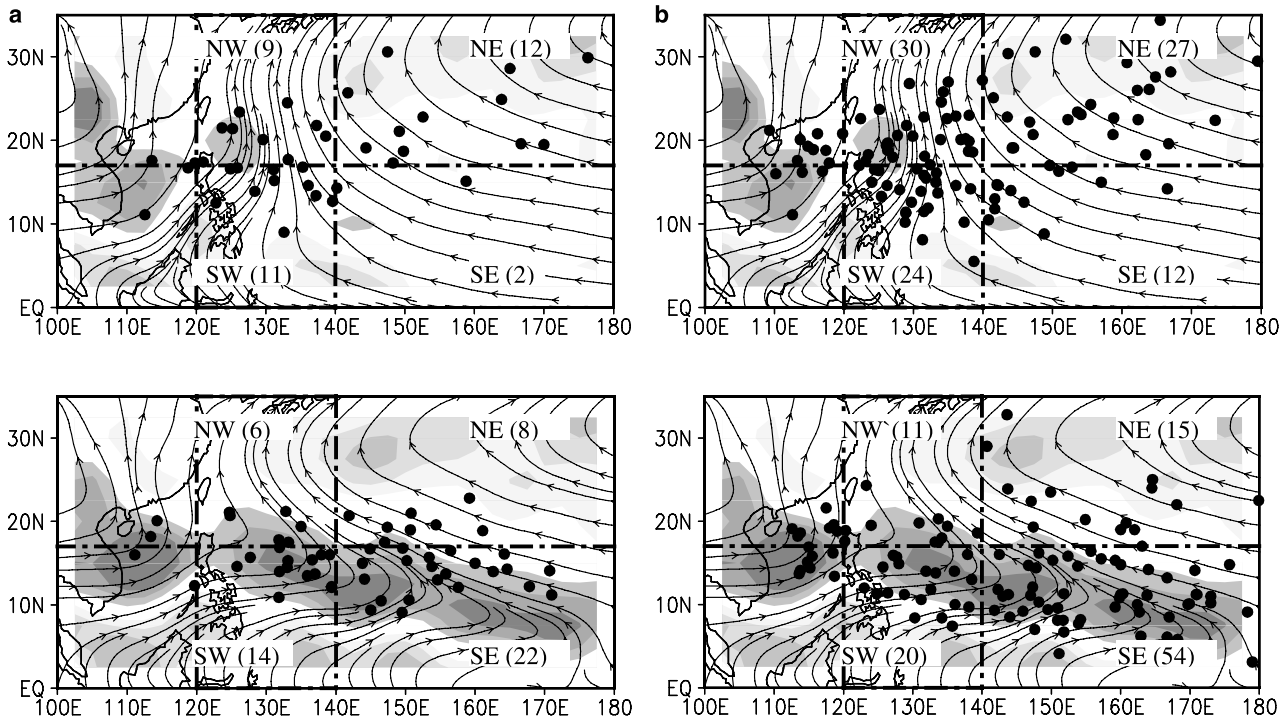

Fig. 6. (**a**) Composite distributions of initial RI positions (dots) during seven strong cold years (upper panel) and seven strong warm years (lower panel). See text for the defined strong warm and cold years. (**b**) The same as in (**a**) except for the initial TC formation positions (dots). The dashed lines divide WNP into four quadrants as in Wang and Chan (2002), namely NW, NE, SW and SE. The numbers in the bracket indicate the total numbers of occurence of RI and TD, respectively, in each quadrant. The meaning of the streamlines and the shading is the same as in Fig. 5.

ENSO impact between the RI and TC formation, we examine composite scenarios with regard to the Niño 3.4 SSTA, which is the sea surface temperature anomalies averaged over the eastern-central Pacific (5° S–5° N, 120° W–170° W)

Figure 6a compares the spatial distributions of the initial locations of RI between seven strong warm and seven strong cold ENSO years in the last 40 years (1965–2004). In the JAS season, seven strong warm years (1965, 1972, 1982, 1987, 1991, 1997, and 2002) and seven strong cold years (1970, 1971, 1973, 1975, 1988, 1998 and 1999) were selected according to the criterion that the absolute value of the Niño 3.4 SSTA in JAS exceeds a unit standard deviation. To facilitate comparison between RI and TC formation, Fig. 6b presents a counterpart of Fig. 6a for the TC formation.

Obviously, similarities exist between Fig. 6a and b. For instance, during the strong warm years, both the TC's RI and its formation tend to shift equatorward and eastward, whereas during the strong cold years, they tend to shift poleward and westward. The meridional shifts of the RI and TC formations are particularly evident. This equatorward shift of the TC formation and RI results from large-scale circulation change associated with the El Niño and La Niña. A detailed discussion of the cause of the changes in the large-scale circulation in the western North Pacific can be found in Wang and Chan (2002) and Lau and Wang (2006) (Chapter 12 the Asian monsoon).

However, important differences exist between the TC's RI and its formation. Over the WNP (120° E–180° E), the mean number of RI in strong warm years is 7.1, which is notably higher than that in strong cold years 4.9. In contrast, the mean numbers of TC formation (including TD) during the seven warm years 14.3 and seven cold years (13.3) tend to be comparable. This indicates that El Niño and La Niña have a more significant impact on the number of RI events than the number of TC formation. As a result, the proportion of TCs with RI is higher (53%) in the warm years while lower (37%) during the cold years. Furthermore, the difference in the northwest (NW) quadrant (17–30° N, 120–140° E) is

more evident. For instance, the number of TC formation is negatively correlated with the Niño 3.4 SSTA with a correlation coefficient of −0.55, while the TC RI does not ($R = -0.1$). This result reflects the fact that when favorable condition shifted northward during La Niña, the TC formation increases, but the RI is not.

What are responsible for the difference between the RI and TC formation in the WNP? First, the most evident difference in seasonal mean circulation between strong developing El Niño and La Niña years is seen in the 850 hPa vorticity field (Fig. 6). During El Niño, the monsoon trough is enhanced and extended southeastward, whereas in developing La Niña years, the WNP monsoon trough nearly disappears. This causes a southward shift of the TC initiation area (Fig. 6b). This shift favors TCs having a longer life span over the warm ocean with abundant heat content and having more chance for RI. During strong La Niña years, favorable conditions for TC formation, i.e., the upper-level divergence anomalies (Wang and Chan, 2002), shifted northward, which may enhance the formation of TCs, but not for RI as much. The reason is that the RI relies on the presence of sufficient mixed-layer heat content more sensitively than formation does because the RI needs a higher rate of latent heat supply than the formation. In a higher latitude, the mixed-layer heat content are in general not favorable for RI unless in the presence of warm eddies (Lin et al, 2005). Further, with increasing latitude, the increased Coriolis parameter tends to enhance the inertial stability and slow down intensification because the low-level inflow cannot reach the inner core region as quickly as that in a low-latitude vortex.

In addition to the latitude factor, we additionally noticed, in the region (13–35° N and 125–150° E) shown by the long dashed box in Fig. 7, that the total number of TCs formed during strong cold years (50) is twice that during strong warm years (25). By contrast, the numbers of RI events are about the same (21 and 20). Thus, the proportion of rapidly intensifying TCs to the total number of TC formation increases from 40% during cold years to 80% during warm years, suggesting that the TCs have less chance of RI in the afore-

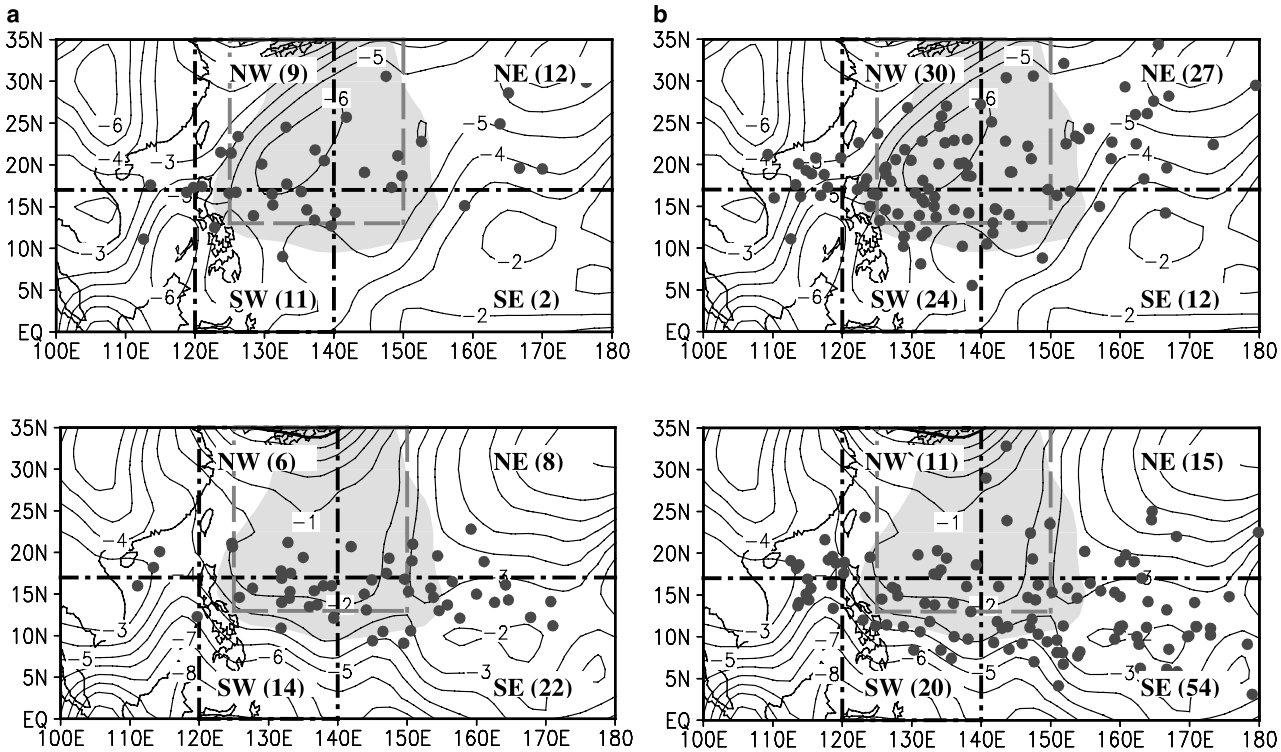

Fig. 7. The same as in Fig. 6 but added large scale environmental vertical shear of meridional winds. The contours represent the magnitude of the vertical shear of the meridonal wind component. The shading indicates statistical significance between strong warm and strong cold years at a 95% confident level using a two-sample *t*-test. The long dashed box indicates the region where the proportion of RI increases from 40% during cold years to 80% during warm years

mentioned region during La Niña years. What is the difference in the large-scale circulation? We noticed that in the aforementioned region, northerly vertical shear is enhanced in La Niña years (the magnitude is 5–6 m/s), whereas it becomes smaller in El Niñoones (the magnitude is only 1–2 m/s) (Fig. 7). The reason is that during El Niño years, the enhanced heating in the central equatorial Pacific induces a Rossby wave response that has anomalous upper-level southerly and low-level northerly in the aforementioned region, thus generating an anomalous southerly vertical shear (upper-level southerly and low-level northerly). During La Niña years the anomalous circulations reverse and enhanced northerly vertical shear prevails in the aforementioned region.

Can the aforementioned large-scale circulation differences cause the change in the proportion of RI? We propose that the increase in environmental northerly vertical shear (northerly increase with height) during La Niña may reduce the chance for RI. Previous investigations have found that the increased vertical shear is unfavorable for TC development (DeMaria, 1996; Molinari et al, 2004). However, the increased total vertical shear would not be only destructive to the RI but also, and perhaps more, destructive to TC formation. Thus, the issue is why the increased northerly vertical shear is more determent to RI than to TC formation. Our interpretation is as follows. An anomalous northerly vertical shear consists of a low-level southerly anomaly and an upper-level northerly anomaly. The low-level anomalous southerly environmental flow favors for a net spin-down of cyclonic circulation due to the increase with latitude of the Coriolis torque, which induces an anticyclonic circulation; at the same time, the upper-level anomalous northerly may cause a net spin-down of anticyclonic circulation (Frank, 1977b). As a result, an anomalous northerly vertical shear would resist the RI of a TC that is normally characterized by a low-level cyclonic circulation and an upper-level anticyclonic circulation (Frank, 1977a). For those TCs that formed during strong La Niña years (shown in the long dashed box in Fig. 7), the opportunity for RI should be reduced, owing to the enhanced northerly wind vertical shear. Because incipient TCs have weak upper-level anticyclonic circulation, it is conceivable that an anomalous environmental northerly shear may have weaker destructive impacts on TC formation than TC rapid intensification.

5.2 Interannual variations of the RI

Figure 8 shows that the number of RI in the entire WNP during the peak season from July to October (JASO) exhibits large interannual variation, ranging from 3 to 13. The 40-year averaged number of rapidly intensifying TCs is 7.8 with a standard deviation of 2.6. The time series of the JASO number of RI events also shows pronounced decadal variations, *but no significant trend* is seen over the past 40 years.

The simultaneous correlation between RI and Niño 3.4 SSTA in the JAS season is statistically significant ($R = 0.32$), but the correlation coefficient is low. By contrast, the correlation coefficient between the TC formation number and Niño 3.4 SSTA (-0.01) is not statistically significant. This confirms the important difference between RI and the formation of TCs in terms of their response to ENSO. The low correlation between RI and Niño 3.4 SSTA indicates that while the ENSO is a factor contributing to the interannual variation of RI, it is not the sole source of the variability. We need to think more broadly. For this purpose, we will contrast the climate anomalies between the active and inactive RI years in a hope that we may find some useful hints for climate prediction of RI and to understand better the climate conditions that affect RI occurrence.

To identify favorable environmental conditions for RI, we examine monthly mean anomalous circulations. For a given calendar month, we

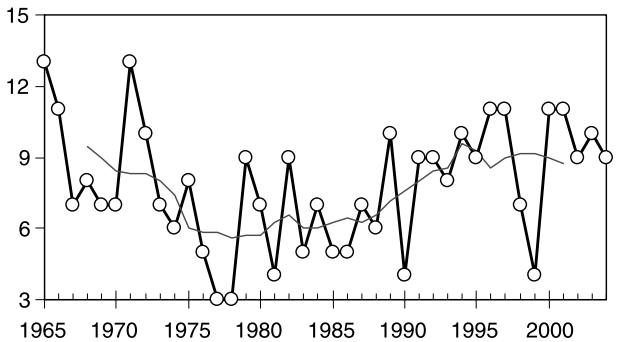

Fig. 8. The time series of the number of TC RI occurring during the peak RI seasons (July–October) in the WNP for the period 1965–2004. Thin curves indicate a five-year running mean, which shows large interdecadal variations but not a linear trend

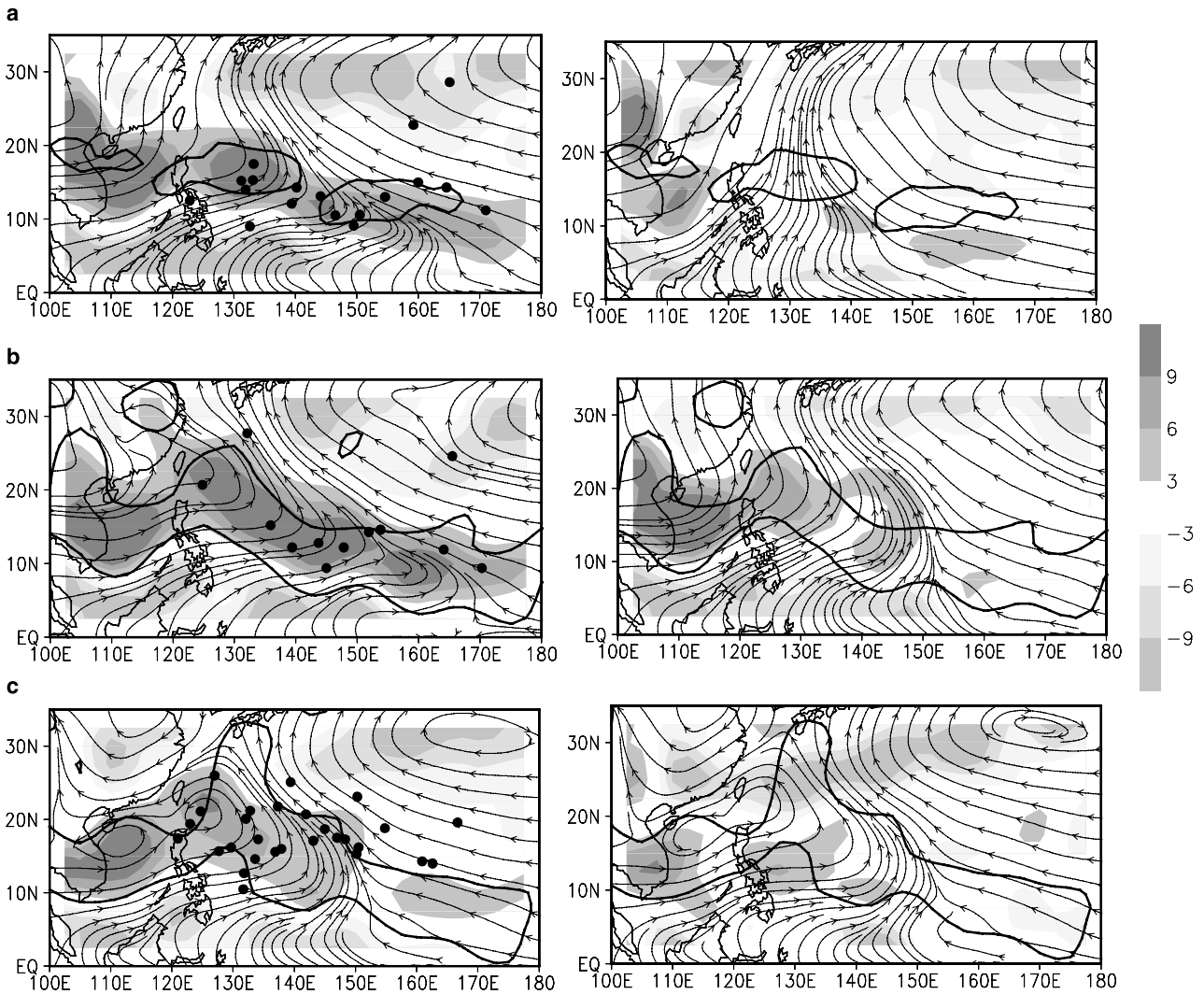

Fig. 9. Composite 850 hPa streamlines and relative vorticity for active (left panel) and inactive (right panel) years for (**a**) July, (**b**) August, (**c**) September. The thick lines outline the regions where the differences between RI active and inactive years are statistically significant at 95% confident level. The years of active and inactive RI are explained in the text

define those years during which no RI occurs as inactive years; and those years that exhibit more than three RI occurrences as active RI years. Composite monthly mean 850 hPa winds and vorticity for active and inactive years are shown in Fig. 9. In July, eighteen RI occurred in four most active years (1965, 1971, 1972, and 2002) but none occurred in the seven inactive years (1970, 1978, 1981, 1985, 1993, 1998, and 1999). The most prominent difference between the two composites for the active and inactive years is the strength of the WNP monsoon trough (Fig. 9a). During the active years, the enhanced monsoon trough provides a strong convergence between westerly monsoon flow and southeast trade winds, which promotes RI activity. In contrast, during inactive years, the monsoon trough disappears and southerly winds prevail over the Philippine Sea. In August 12 RI events occurred in three most active years (1982, 1992, and 2004), while none in the seven inactive years (1969, 1972, 1973, 1977, 1978, 1986, and 1991). The differences between the active and inactive years' composite low-level circulation are similar to that in July (Fig. 9b). September is the month in which TC RI is most active (see Fig. 2a). Twenty-eight RI events occurred in seven active RI years (1965, 1968, 1971, 1979, 1991, 1996, and 2001) and only two years (1973 and 1984) have no RI. However, the differences in 850 hPa wind fields between the two composites are not as clear as in July and August (Fig. 9c). Never-

theless, the vorticity differences remain significant between the active and inactive years. In addition to the low-level condition, the 200 hPa divergence differences between active and inactive years were contrasted for each peak season month. There are some indications of the linkage between enhanced upper-level divergence and the increased RI in July but not in August and September (not shown).

6. Intraseasonal and seasonal prediction of RI

6.1 Intraseasonal prediction

The simultaneous relationship shown in Fig. 5 cannot be used for prediction unless the intraseasonal oscillation over the western North Pacific can be faithfully predicted in advance. Thus, it is desirable to search for precursors for RI. This is possible because the previous studies have found a tendency for ISO anomalies to propagate northwestward from the equatorial Western Pacific (EWP) during boreal summer (Lau and Chan, 1986; Wang and Rui, 1990; Kemball-Cook and Wang, 2001). As shown in Fig. 10 adopted from Kemball-Cook and Wang (2001), the northwestward propagation of ISO anomalies provides a potential precursory condition for prediction of the ISO in the WNP during July, August, September, and October.

Therefore, we define an EWP ISO index by averaging the 30–60-day filtered OLR anomalies over the EWP (5° S–5° N, 140–160° E). A total of 55 large-amplitude events with a mean period of 33 days were identified and selected during July–October from 1979 to 2004 according to the time series of the EWP ISO index. The amplitudes of each event selected are greater than 0.9 standard deviations. Since the periods of individual cycles are irregular, the method used to construct the composite life cycle was based on eight consecutive phases in each of the 55 cycles, following Wang et al (2006). Phases 1, 3, 5, and 7 correspond to, respectively, the time when OLR anomalies are at a minimum, a positive transition phase (negative-turning-to-positive), a maximum, and a negative transition phase. Thus, Phases 1 and 5 represent, respectively, the wettest and the driest phases in the EWP. Since the mean period of ISO is 33 days, each phase spans about 4 days.

Figure 11 shows the dependence of the RI occurrence in the South China Sea and Philippine Sea (SCS–PS: 10–20° N, 110–150° E) on the ISO phases in the EWP. The mean frequency of the RI occurrence shows a pronounced ISO cycle. The maximum frequency of RI in Phase 4 is more than five times than that the minimum frequency in Phase 8. The peak phase of RI over the WNP occurs in Phase 4, which lags behind the ISO wettest phase in the EWP (Phase 1) by three phases (about 12 days). It indicates that the ISO activity over the EWP can indeed be used in the subseasonal prediction of the RI activity over the

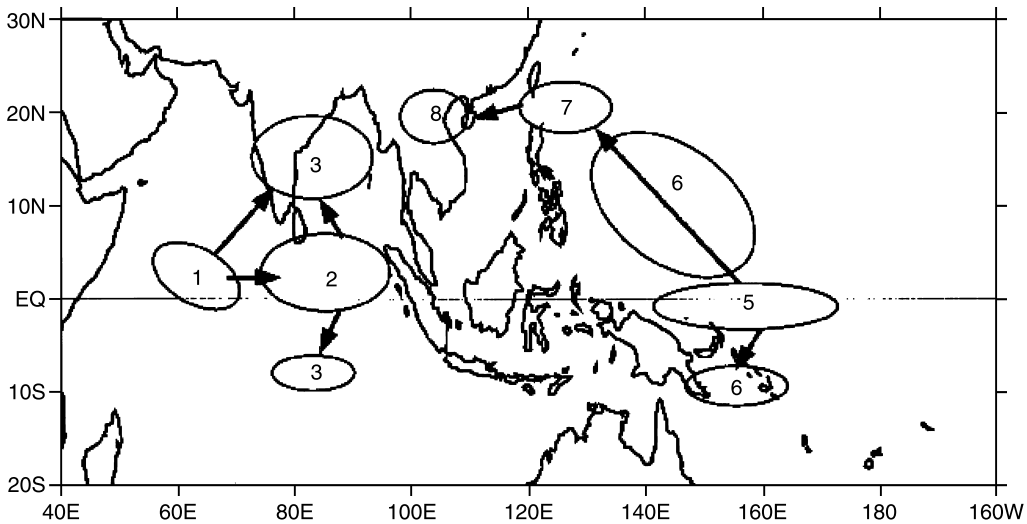

Fig. 10. A schematic diagram showing the life cycle of the intraseasonal convective anomalies for the August–September–October season. The numbers denotes the composite phases of ISO. Adopted from Kemball-Cook and Wang (2001)

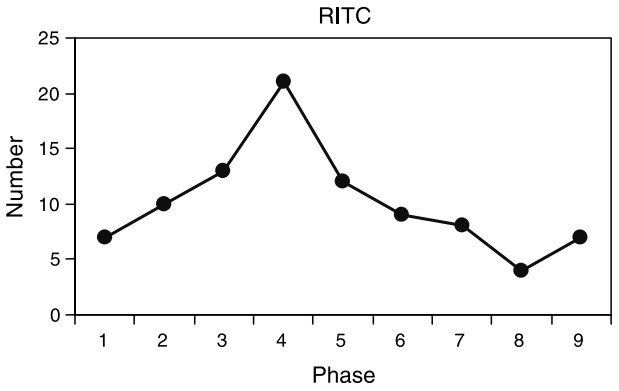

Fig. 11. The number of RI that occurred over the South China Sea and Philippine Sea (SCS–PS: 10–20° N, 110–150° E) as a function of the composite phases of ISO in the equatorial western Pacific (EWP: 5° S–5° N, 140° E–160° E). The composite was made based on 55 cases of ISO in the EWP during June through October. Phases 1 and 5 represent, respectively, the strongest and weakest convection phases over the EWP. Thus, the maximum occurrence of RI over the SCS–PS lags the peak wet phase of the EWP ISO by three phases (about 12 days) and the minimum occurrence of RI over the SCS–PS lags the peak wet phase of the WNP ISO by seven phases (about 28 days)

South China Sea and Philippine Sea (10–20° N, 110–150° E). It takes about 12 days for the most intense convection in the EWP to reach South China Sea and Philippine Sea, and this intense convection modulates RI. Note also that a minimum in RI in the South China Sea and Philippine Sea occurs in Phase 8, which lags behind the wettest phase of the EWP ISO by about 28 days, providing a long-lead predictor for intraseasonal forecast of the RI.

6.2 Seasonal prediction

The results shown in Fig. 6 suggest that seasonal prediction of RI can be better made if we consider a specific region in the WNP rather than looking at the entire WNP. Figure 12 shows that the number of RI in the SE quadrant (0–17° N, 140–180° E) during JAS season is well correlated with the Niño 3.4 SSTA anomalies in June, just before the peak season of RI. The correlation coefficient is 0.63 for the period of 1965–2004. Thus, the Niño 3.4 SSTA in June can serve as a predictor for RI in the following three months (JAS) in the SE quadrant of the WNP. It should be mentioned that the RI outside of the SE quadrant is not significantly correlated with June Niño 3.4 SSTA.

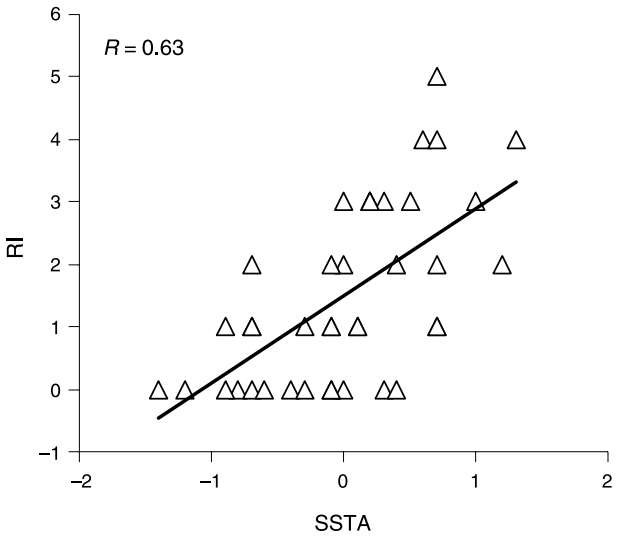

Fig. 12. Scattering diagram showing the dependence of the number of RI in the southeast quadrant of the western North Pacific (0–17° N, 140–180° E) during JAS (ordinate) on the June Niño 3.4 SSTA anomalies (abscissa)

7. Summary and discussion

One of the major purposes of the present investigation was to identify climatic conditions that may control the frequency and location of tropical cyclone (TC) rapid intensification (RI) over the western North Pacific (WNP) on annual, intraseasonal, and interannual time scales. This information is valuable for linking large scale circulation anomalies to RI, thus will be useful for prediction of RI by using general circulation models that can only predict circulation anomalies.

Particular attention was paid to a comparison of RI with TC formation process. The RI and TC formation share many common environmental preferences. For instance, the RI and TC incipience increase proportionally during a period of enhanced monsoon trough associated with the intraseasonal oscillation (Fig. 5 and Table 1); and both the RI and TC formation are enhanced in the southeast quadrant of the WNP during El Niño years (Fig. 7a and b).

While the RI and TC formation share common environmental preferences, we found a number of interesting differences in the climate factors controlling their annual and interannual variations. In annual cycle, the greatest number of TCs form in August, when the warm water and monsoon trough extend to their northernmost positions and often, a huge monsoon gyre controls the WNP (Lander, 1994b). However, only 30% of

the total number of TCs actually experience RI in August in comparison to 47% in November (Fig. 3). During the peak TC season (July–August–September), the RI activity is enhanced during El Niño years and suppressed during La Niña years; however, the TC formation number does not differ significantly between the El Niño and La Niña years (Fig. 6). Further, during La Niña years, while more TCs develop in the northwest quadrant (17–30° N, 120–140° E) and the northeast quadrant, the RI is not enhanced significantly there (Fig. 6).

We propose that three factors may be responsible for explaining the differences in the favorable climate conditions for the RI and formations. First, the latitudinal location and ocean mixed-layer heat content can make differences between the RI and TC formation. Figure 13 shows how the proportion of RI (the ratio of TCs with RI to total number of tropical storms) varies as a function of mean latitude where TCs form. On annual cycle, it is obvious that when monthly mean latitude of TC formation is low, the corresponding proportion of RI tends to be high (Fig. 13a). This is also valid on the interannual time scale (Fig. 13b). When seasonal (July–August–September) mean latitude of tropical storm formation in an individual year is low, the corresponding proportion of seasonal RI events tend to be high ($R = -0.47$ for a 40-year sample). The dependence of the proportion of RI on latitude is a robust signal. Our interpretation of this relationship follows. When the mean latitude of tropical storm formation increases the mixed-layer heat content decreases; thus it cannot sustain the high rate of latent heat supply that RI demands. Further, as latitude increases, the RI process weakens because the increasing Coriolis parameter tends to increase inertial stability of the TC circulation and slow down the low-level radial inflow. Both the decrease in the mixed layer heat content and increase in inertial stability are more detrimental to RI than to the TC formation as RI requires a much more efficient secondary circulation that supplies latent energy from the ocean surface (Emanuel, 1986).

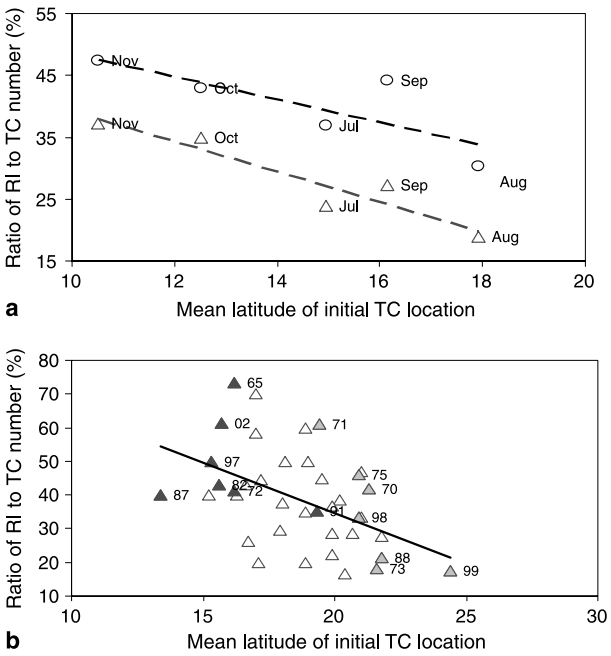

Fig. 13. Scattering diagrams showing (**a**) the dependence of the proportion of RI as a function of calendar month (circle) on mean latitude of initial TC formation location on annual time scale. The triangles represent a more restricted RI definition using a threshold value of 40 knots per 24 hours. (**b**) The dependence of RI on mean latitude of initial TS location during the period from July to September of each year. Heavy (light) shading represent strong warm (cold) years. The white triangles stand for normal years

Second, the cyclonic shear of the low-level environmental westerly flow is important. While the monsoon gyre in August provides a favorable environment for TC formation, it is not conducive to RI. This is because the cyclonic shear of the ambient zonal flow is lowest in August (but highest in November) (Fig. 4). On the interannual time scale, the active RI years are also characterized by enhanced low-level westerly meridional shear vorticity (Fig. 9). The mechanism has been discussed in Sect. 4. We believe that the cyclonic environmental shear-induced wavenumber two asymmetric circulation in the TC inner core region favors for intensification through axisymmetrization. This axisymmetrization process is more effective to increase of intensification rate than TC formation.

Third, an anomalous northerly vertical shear resists RI of a TC due to the opposing effects of the Coriolis torque exerting on the TC circulation. This detrimental impact is more severe to RI than to formations, because the net spin down of TC circulation by an anomalous northerly shear occurs in both the lower and upper levels for the RI process while it is primarily confined to the lower level for the formations.

In summary, the increasing low-level westerly meridional shear vorticity and decreasing north-

erly vertical shear in the latitudes between 8° N and 20° N provide the most favorable environmental conditions for RI (or supper typhoons).

Another purpose of the present study is to identify predictors for intraseasonal and seasonal prediction of RI in the WNP. Admittedly, the simultaneous relationships between RI activity and environmental preferences, while shed light on understanding physical mechanisms, have little value for prediction. An effort has been made to search for useful predictors of RI in Sect. 6. The results shown in Fig. 11 indicate that the intraseasonal oscillation in the equatorial western Pacific (5° S–5° N, 130–150° E) can be useful in predicting the RI activity in the Philippine Sea and South China Sea about 10 to 30 days in advance. The results, shown in Fig. 12, are valuable for prediction of seasonal mean strength of RI activity in terms of Niño 3.4 SSTA.

The results derived from this study have important implication for understanding changes of TC intensity in a warming environment. As pointed out in the Sect. 3, about 90% of the super typhoons underwent at least one RI process during their lifespans. Over the Atlantic, all category 4 and 5 hurricanes experience at least one RI processes in their lifespans (DeMaria and Kaplan, 2003). Therefore, the favorable climate conditions for RI also apply to the development of super typhoons in the WNP and perhaps the category 4 and 5 hurricanes in Atlantic. Over the past 40 years, the annual total of RI in the western North Pacific shows pronounced interdecadal variation but no significant trend. This implies that the supper typhoons had likely no upward trend in the last 40 years.

What control the proportion of super typhoons or hurricanes? We infer that when the mean latitude, where the tropical storms form, shifted southward (either seasonally or from year to year) the proportion of super typhoon or major hurricane will increase. This finding contrasts the current notion that higher SST leads to more frequent occurrence of category 4 or 5 hurricanes (Emanuel, 2005; Webster et al, 2005). The major reason is that it is the ocean mixed layer heat content rather than SST that determines the RI process, which is a process that every intense hurricane or supper typhoon must go through. In the global warming condition, whether the proportion of major hurricane will increase should largely depend on how the changing atmospheric conditions shift the locations of the tropical cyclone formation.

The present analysis was confined to atmospheric conditions. Obviously that is not sufficient. As we speculated, the ocean mixed layer heat content can be a critical factor that determines the RI. Further quantification of the relationship between the heat content anomalies and RI activity are undertaking. In addition, the possible roles of higher lower-troposphere relative humidity and associated thermodynamic conditions deserve further careful examination. The physical mechanisms proposed in the present study demand further verification through numerical experiments.

Acknowledgements

The authors thank valuable comments made by Dr. Liguang Wu on an earlier version of the manuscript. U.S. Office of Naval Research under Grant N00014-021-0532 supported this work. This is School of Ocean and Earth Science and Technology publication number 7038 and International Pacific Research Center publication number 428.

References

Bister M (2001) Effect of peripheral convection on tropical cyclone formation. J Atmos Sci 58: 3463–3476

Brand S (1973) Rapid intensification and low-latitude weakening of tropical cyclones of the western North Pacific Ocean. J Appl Meteorol 12: 94–103

Chan JCL (1985) Tropical cyclone activity in the Northwest Pacific in relation to the El Niño/Southern Oscillation phenomenon. Mon Wea Rev 113: 599–606

Chen T-C, Weng S-P, Yamazai N, Kiehne S (1998) Interannual variation in the tropical cyclone formation over western North Pacific. Mon Wea Rev 126: 1080–1090

DeMaria M (1996) The effect of vertical shear on tropical cyclone intensity change. J Atmos Sci 53: 2047–2087

DeMaria M, Pickle JD (1988) A simplified system of equations for simulation of tropical cyclones. J Atmos Sci 45: 1542–1554

DeMaria M, Zehr RM, Kossin JP, Knaff JA (2002) The use of GOES imagery in statistical hurricane intensity prediction. 25th Conf. on Hurricanes and Tropical Meteorology, San Diego, CA. Amer Meteor Soc, pp 120–121

Dvorak VF (1975) Tropical cyclone intensity analysis and forecasting from satellite imagery. Mon Wea Rev 103: 420–430

Emanuel KA (1986) An air-sea interaction theory for tropical cyclones. Part I: Steady-state maintenance. J Atmos Sci 43: 585–604

Emanuel KA (2005) Increasing destructiveness of tropical cyclones over the past 30 years. Nature 436: 686–688

Frank WM (1977a) The structure and energetics of the tropical cyclone I. Storm structure. Mon Wea Rev 105: 1119–1135

Frank WM (1977b) The structure and energetic of the tropical cyclone II. Dynamics and energetics. Mon Wea Rev 105: 1136–1150

Gray WM (1968) Global view of the origin of tropical disturbances and storms. Mon Wea Rev 96: 669–700

Gray WM (1984) Atlantic seasonal hurricane frequency. Part I: El Niño and 30 mb quasi-bieniial osillation influences. Mon Wea Rev 112: 1649–1668

Gray WM (1998) The formation of tropical cyclones. Meteorol Atmos Phys 67: 37–69

Gross JM (2001) North Atlantic and East Pacific track and intensity verification for 2000. Minutes of the 55th Interdepartmental Hurricane Conf., Miami, FL, Office of the Federal Coordinator for Meteorological Services and Supporting Research, NOAA, B12–B15. [Available from Federal Coordinator for Meteorological Services and Supporting Research, 6101 Executive Blvd, Ste. 900, Rockville, MD 20852]

Hall JD, Mathews AJ, Karoly DJ (2001) The modulation of tropical cyclone activity in the Australian region by Madden-Julian Oscillation. Mon Wea Rev 129: 2970–2982

Harr PA (2006) Temporal clustering of tropical cyclone occurrence on intraseasonal time. 27th Conf. on Hurricanes and Tropical Meteorology, Monterey, CA. Amer Meteor Soc, 3D.2

Hendon HH, Liebmann B (1994) Organization of convection within the Madden-Julian oscillation. J Geophys Res 99: 8073–8083

Holland GJ (1995) Scale interaction in the western Pacific monsoon. Meteor Atmos Phys 56: 57–79

Holliday CR, Thompson AH (1979) Climatological characteristics of rapidly intensification typhoons. Mon Wea Rev 107: 1022–1034

Hsu H-H, Lo A-K, Hung C-H, Wu C-C (2006) Possible feedback of tropical cyclone on climate variability. 27th Conf. on Hurricanes and Tropical Meteorology, Monterey, CA. Amer Meteor Soc, 11C.6

Jones C, Carvalho LMV, Higgins RW, Waliser DE, Schemm J-KE (2004) Climatology of tropical intraseasonal convective anomalies: 1979–2002. J Climate 17: 523–539

Kaplan J, DeMaria M (2003) Large-scale characteristics of rapidly intensifying tropical cyclones in the north Atlantic basin. Wea Forecast 18: 1093–1108

Kemball-Cook S, Wang B (2001) Equatorial waves and air-sea interaction in the boreal summer intraseasonal oscillation. J Climate 14: 2923–2942

Lander MA (1994a) An exploratory analysis of the relationship between tropical storm formation in the western North Pacific and ENSO. Mon Wea Rev 122: 636–651

Lander MA (1994b) Description of a monsoon gyre and its effects on the tropical cyclones in western North Pacific during August 1991. Wea Forecast 9: 640–654

Landsea CW (2000) El Niño/Southern Oscillation and the Seasonal Predictability of Tropical Cyclones. In: El Niño and the Southern Oscillation: multiscale variability and global and regional impacts (Diaz HF, Markgraf V, eds). Cambridge University Press, pp 149–181

Lau KM, Chan PH (1986) Aspects of 40–50 day oscillation during the northern summer as inferred from outgoing longwave radiation. Mon Wea Rev 114: 1354–1367

Lau N-C, Wang B (2006) Interactions between the Asian monsoon and the El Niño/Southern Oscillation. In: The Asian Monsoon, Berlin: Praxis, 479–511

Li X, Wang B (1996) Acceleration of the hurricane beta drift by shear strain rate of an environmental flow. J Atmos Sci 53: 327–334

Liebmann B, Hendon HH, Glick JJ (1994) The relationship between tropical cylones of the Western Pacific and Indian Oceans and the Madden-Julian Oscillation. J Meteor Soc Japan 72: 401–412

Lin I-I, Wu C-C, Emanuel KA, Lee I-H, Wu C-R, Pun I-F (2005) The interaction of Supertyphoon Maemi (2003) with a warm ocean Eddy. Mon Wea Rev 133: 2635–2649

Maloney ED, Hartmann DL (2000) Modulation of eastern North Pacific hurricanes by the Madden-Julian oscillation. J Climate 13: 1451–1460

Maloney ED, Hartmann DL (2001) The Madden-Julian oscillation, barotropic dynamics, and north Pacific tropical cyclone formation. Part I: Observation. J Atmos Sci 58: 2545–2558

Molinari J, Vollaro D, Corbosiero KL (2004) Tropical cyclone formation in a sheared environment: a case study. J Atmos Sci 61: 2493–2509

Montgomery MT, Enagonio J (1998) Tropical cyclogenesis via convectively forced vortex Rossby waves in three-dimensional quasi–geostrophic model. J Atmos Sci 55: 3176–3207

Nakazawa T (1988) Tropical super clusters within intraseasonal variations over the western Pacific. J Meteor Soc Japan 66: 823–839

Ventham JD, Wang B (2007) Large scale flow patterns and their influence on the intensification rates of western north Pacific tropical stroms. Mon Wea Rev (in press)

Wang B, Chan JCL (2002) How strong ENSO events affect tropical storm activity over the western North Pacific. J Climate 15: 1643–1658

Wang B, Fan Z (1999) Choice of south Asian summer monsoon indices. Bull Amer Meteor Sci 80: 629–638

Wang B, Rui H (1990) Synoptic climatology of transient tropical intraseasonal convection anomalies: 1975–1985. Meteorol Atmos Phys 44: 43–61

Wang B, Wu R, Lau K-M (2001) Interannual variability of Asian summer monsoon: contrast between the Indian and western North Pacific–West Asian monsoon. J Climate 14: 4073–4090

Wang B, Ho L, Zhang Y, Lu M-M (2004) Definition of South China Sea monsoon onset and commencement of East Asia summer monsoon. J Climate 17: 699–710

Wang B, Webster P, Kikuchi K, Yasunari T, Qi Y (2006) Boreal summer quasi–monthly oscillation in the global tropics. Clim Dynam (DOI: 10.1007/s00382-006-0163-3)

Webster PJ, Holland GJ, Curry JA, Chang HR (2005) Changes in tropical cyclone number, duration, and intensity in a warming environment. Science 309: 1844–1846

Wu L, Wang B (2004) Assessing impacts of global warming on tropical cyclone tracks. J Climate 17: 1686–1698

Corresponding author's address: Bin Wang, Department of Meteorology, University of Hawaii, 2525 Correa Rd., Honolulu, Hawaii 96822, USA (E-mail: wangbin@hawaii.edu) (also visiting professor at the Ocean University of China)